



HAL
open science

Guided acoustic wave resonators using an acoustic Bragg mirror

I. Kone, F. Domingue, H. Jacquinot, M. Borel, M. Gorisse, A. Reinhardt, G. Parat, F. Casset, D. Pelissier-Tanon, J.F. Carpentier, et al.

► **To cite this version:**

I. Kone, F. Domingue, H. Jacquinot, M. Borel, M. Gorisse, et al.. Guided acoustic wave resonators using an acoustic Bragg mirror. *Applied Physics Letters*, 2010, 96 (22), pp.223504. 10.1063/1.3440370 . hal-00548560

HAL Id: hal-00548560

<https://hal.science/hal-00548560>

Submitted on 30 May 2022

HAL is a multi-disciplinary open access archive for the deposit and dissemination of scientific research documents, whether they are published or not. The documents may come from teaching and research institutions in France or abroad, or from public or private research centers.

L'archive ouverte pluridisciplinaire **HAL**, est destinée au dépôt et à la diffusion de documents scientifiques de niveau recherche, publiés ou non, émanant des établissements d'enseignement et de recherche français ou étrangers, des laboratoires publics ou privés.

Guided acoustic wave resonators using an acoustic Bragg mirror

Cite as: Appl. Phys. Lett. **96**, 223504 (2010); <https://doi.org/10.1063/1.3440370>

Submitted: 26 February 2010 • Accepted: 29 April 2010 • Published Online: 03 June 2010

I. Koné, F. Domingue, A. Reinhardt, et al.



View Online



Export Citation

ARTICLES YOU MAY BE INTERESTED IN

[High quality factor surface Fabry-Perot cavity of acoustic waves](#)

Applied Physics Letters **112**, 073505 (2018); <https://doi.org/10.1063/1.5013161>

[High performance AlScN thin film based surface acoustic wave devices with large electromechanical coupling coefficient](#)

Applied Physics Letters **105**, 133502 (2014); <https://doi.org/10.1063/1.4896853>

[High performance lithium niobate surface acoustic wave transducers in the 4–12GHz super high frequency range](#)

Journal of Vacuum Science & Technology B **33**, 06F401 (2015); <https://doi.org/10.1116/1.4935561>

Lock-in Amplifiers
up to 600 MHz



Zurich
Instruments



Guided acoustic wave resonators using an acoustic Bragg mirror

I. Koné,^{1,a)} F. Domingue,^{1,b)} A. Reinhardt,^{1,c)} H. Jacquinet,¹ M. Borel,¹ M. Gorisse,¹ G. Parat,¹ F. Casset,¹ D. Pellissier-Tanon,² J. F. Carpentier,² L. Buchailot,³ and B. Dubus³

¹CEA, Leti, Minatec, F-38054 Grenoble, France

²FTM-Crolles, STMicroelectronics, F-38920 Crolles, France

³IEMN, Département ISEN, UMR CNRS 8520, Lille F-59046, France

(Received 26 February 2010; accepted 29 April 2010; published online 3 June 2010)

Lamb wave devices have recently gained an interest for providing narrow bandpass filters in wireless transmission systems. Their cointegration with film bulk acoustic wave resonators is a major advantage, enabling the possibility to provide simultaneously several radio frequency and intermediate-frequency filters in a single fabrication. Similarly, in this work, we report the fabrication of resonators using waves guided in a piezoelectric layer deposited atop a Bragg mirror. Such waves exhibit a behavior close to Lamb waves, thanks to the acoustic isolation provided by the mirror, while being cointegrated along with solidly mounted resonator structures. © 2010 American Institute of Physics. [doi:10.1063/1.3440370]

Lamb wave devices have recently gained an interest for wireless transmission systems, where narrow bandpass filters for channel selection at intermediate frequency (IF) are required.^{1–6} Compared to surface acoustic waves (SAW), Lamb wave resonators may be fabricated atop silicon substrates and are thus more easily integrated in radio-frequency (rf) circuits. Moreover, it has been shown that Lamb wave resonators based on aluminum nitride (AlN) membranes can be cointegrated with film bulk acoustic resonators in order to provide both IF and rf filters on the same chip,⁷ saving significant space and reducing assembly costs.

Several groups have almost simultaneously reported the possibility to exploit waves propagating in a piezoelectric waveguide and confined through the use of an acoustic Bragg mirror,⁸ providing resonators similar to Lamb wave resonators while using a technology compatible with solidly mounted resonators (SMR). This has been seen as a way to exploit high velocity SAW at high frequencies when using an omnidirectional mirror, hence the term OMNISAW.⁹ A similar concept has arisen from the observation that a lateral acoustic coupling between SMR may be obtained by exploiting laterally propagating waves which are often seen as unwanted vibrations in such resonators.¹⁰ Unfortunately, no implementation has been presented for either case. In this work, we report the design, fabrication and characterization of such resonators.

The principle of guided wave resonators is to use a piezoelectric thin film, in our case AlN as a waveguide and to provide an acoustic confinement using an air/solid interface on one side, and an acoustic Bragg mirror on the other. This mirror is made for example of silicon oxycarbide (SiOC) and silicon nitride (SiN), which stand, respectively, for the low and high acoustic impedance materials. Waves are excited by electrodes deposited on both sides of the piezoelectric film to generate an electric field along the *c*-axis of AlN. The bottom

electrode is implemented as a floating metallic plane, while the top electrode is patterned to form an interdigitated transducer (IDT) with a period corresponding to half a wavelength. This IDT excites a mode very similar to the second symmetric Lamb mode (S1) which would exist in a simple AlN plate of the same thickness, similarly to Ref. 6. To define a resonant cavity, the piezoelectric film is patterned, assuming that limiting the piezoelectric layer provides a sufficient reflexion coefficient, to form a cavity with a limited length of an integer number of half a wavelength.

For optimum confinement, conventional Bragg mirrors are made of quarter-wavelength layers. However, waves guided in the piezoelectric layer can be mathematically expressed as the linear superposition of two plane waves polarized in the sagittal plane, if one neglects vibration out of this plane. Thus, it is necessary to provide a high degree of isolation for each of these plane waves, which exhibit, respectively, a quasilongitudinal and a quasishear polarizations, with a ratio of these two bulk waves velocities close to two. In this case, a quarter-wavelength mirror would only be efficient for one polarization, while showing a large transmission for the other one. Therefore, a three-paired Bragg mirror efficiently isolating both longitudinal and shear polarizations was designed using the scattering matrix method.¹¹ Its transmission coefficients, calculated for a guided wave velocity of 32 km/s (corresponding to a wave excited by a set of interdigitated fingers with a period of 8.4 μm), are shown in Fig. 1. Such a Bragg mirror is very similar, in principle, to the optimized Bragg mirrors used in traditional SMR for optimum energy trapping.¹² The design is only marginally affected by the consideration of a lateral wave propagation, since the mirror transmission does not strongly depend on phase velocity.

Resonators were fabricated as follows: first, the three pairs of SiN(500 nm)/SiOC(1 μm) are deposited on high resistivity silicon wafers by chemical vapor deposition (CVD). They provide a smooth surface (roughness below 2 nm rms) on which to grow the piezoelectric stack. Then, a 300 nm thick bottom molybdenum electrode is sputtered and patterned using a fluorine-based dry etching, to define the bottom floating electrode. AlN (1.7 μm) is deposited by re-

^{a)}Also at IEMN département ISEN, UMR CNRS 8520, Lille, France and at FTM-Crolles, STMicroelectronics, F-38920 Crolles, France.

^{b)}Now with the Laboratoire des microsystèmes et télécommunications (LMST), Département de génie électrique et génie informatique, Université du Québec à Trois-Rivières, Trois-Rivières, QC G9A 5H7, Canada.

^{c)}Electronic mail: alexandre.reinhardt@cea.fr.

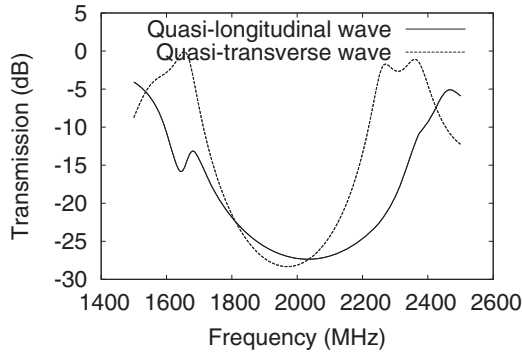


FIG. 1. Transmission of a three paired SiN/SiOC Bragg mirror for longitudinal (continuous line) and transverse plane waves (dashed line) for a guided wave velocity of 32 km/s.

active pulsed DC sputtering, followed by the deposition of the top molybdenum electrode (300 nm) in the same cluster tool. Top electrodes are then patterned to define interdigitated electrodes with periods of 8.4 or 10 μm and a metallization ratio of 0.5. Then the piezoelectric film is patterned to define the edges of the resonant cavity. A passivation film, protecting the electrodes from oxidation, made of 200 nm SiN encapsulates the top of the resonator as well as its edges. This layer is opened by a fluorine based dry-etching to form vias toward the top electrodes. Finally, a thick aluminum layer is deposited and patterned to cover vias, to form contact pads for rf probing and to decrease the access resistance.

Resonators have been tested on wafer using rf probes connected to a vector network analyzer. The capacitive and inductive contribution of the access lines have been removed, by subtracting the measurement of identical devices without IDT and by estimating the series inductance from high frequency measurements, where this inductance dominates the impedance. Extracted intrinsic resonator characteristics are given in Table I, for a resonator with a set of 30 interdigitated fingers and a period of 8.4 μm . The corresponding electrical response is shown in Fig. 2, along with the simulated harmonic admittance.¹³ A good agreement between measurement and simulation is obtained for the main resonance and for the low frequency spuri. Only the parasitics around 2 GHz differ from simulation, what is attributed to internal reflections at the edges of the top electrodes, which are not taken into account by harmonic admittance calculations. However, the quality factors are still lower than expected from the good transmission characteristics shown in Fig. 1 for both longitudinal and shear polarizations. The roughness of the Bragg mirror layers should also not be responsible for the measured losses, since it remains below 2 nm rms, what is a common target used for SMR resonators which are able to reach quality factors in excess of 800. Instead, we think that losses are partially due to the fact that the exploited mode shows a rather high penetration depth inside the Bragg mirror, as revealed from the displacement

TABLE I. Electrical characteristics of a 30 fingers guided wave resonator.

Resonance frequency	1830 MHz
Antiresonance frequency	1845 MHz
Effective electromechanical coupling factor	2.0%
Quality factor at resonance	160
Quality factor at antiresonance	200

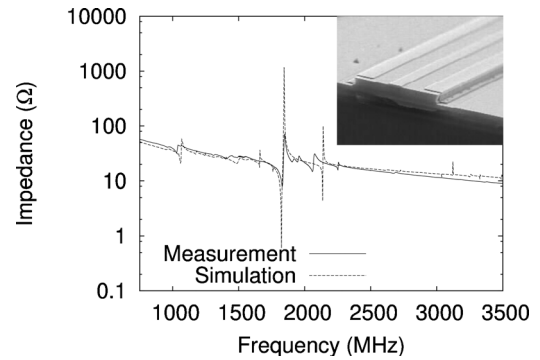


FIG. 2. Electrical response of a guided wave resonator (continuous line), compared to simulations (dashed line). Inset is a SEM view of a resonator with three fingers as its top electrode.

profile shown in Fig. 3. In this figure, one can notice rather large displacement fields in the two first SiOC layers, which are known to exhibit rather high acoustic losses.¹⁴ Therefore, redesigning the Bragg mirror to minimize penetration of the exploited mode would improve the quality factor. Another cause for losses could be the generation of unwanted surface or guided modes inside and outside of the resonator because of mode conversions at the edges of the resonant cavity, where the exploited mode only cannot alone fulfill the stress free boundary conditions.¹⁵

One of the major advantages of guided wave resonators is their ability to adjust the resonance frequency by a proper geometric design of the interdigitated electrodes. This is both caused by a change in wavelength when varying the period of the IDT and by the dispersive nature of the exploited waves. In Fig. 4 we plot the measured frequency variations in measured devices for various IDT periods along with the theoretical dispersion curve. As can be seen, there is again a fair matching between calculations and measurements and a trend to decrease the frequency with decreasing IDT period,

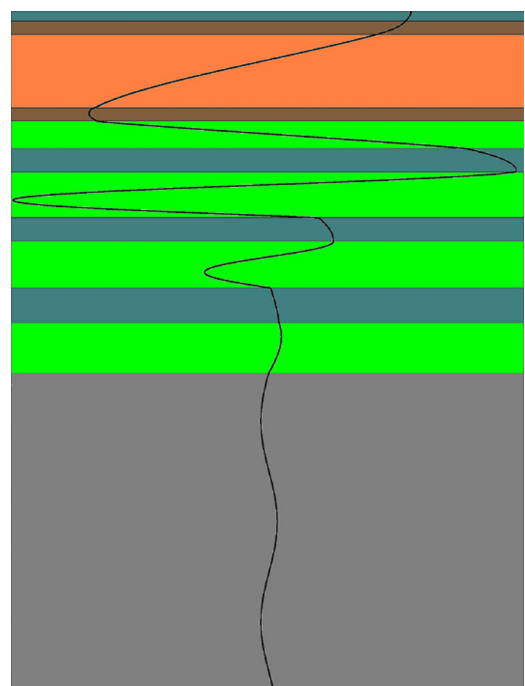


FIG. 3. (Color online) Displacement profile of the guided mode at resonance.

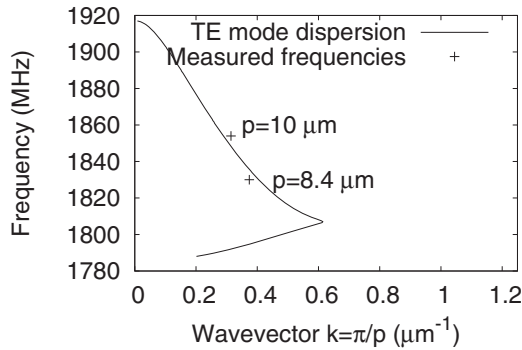


FIG. 4. Dispersion curve for a partially metallized guided wave resonator stack. Points indicate the effective wavevector/frequency of the fabricated resonators.

due to a decrease in wave velocity with wavelength. This trend could be easily modified and even reversed by slightly changing the thicknesses of the Bragg mirror.¹⁶

To demonstrate the possible cointegration of BAW resonators along with guided wave resonators, SMR from the same fabricated wafer have also been measured. They exhibit a resonance frequency of 1860 MHz, corresponding to the cut-off frequency of the thickness-extensional mode, shifted with respect of the dispersion curve of Fig. 4 because of the mass loading of the fully metallized surface. Their effective electromechanical coupling factor of 2%, close to theoretical predictions, is due to the fact that for this fabrication the material stack was only designed for guided wave resonators: the top layer of the Bragg mirror exhibits a significant deviation from a quarter wavelength, decreasing the effective coupling factor of the thickness mode. Again, redesigning the Bragg mirror could make these SMR reach an effective coupling factor of close to 7%. The quality factors at resonance and antiresonance of, respectively, 320 and 250, close to those obtained for guided wave resonators, confirm the hypothesis of absorption by SiOC layers, and could also be improved by a redesign of the material stack, mostly layer thicknesses.

To conclude, this work reports the design and the fabrication of an acoustic resonator exploiting waves guided in a piezoelectric layer isolated from the substrate by the use of a Bragg mirror. Such a device exploits a vibration mode very similar to the SMR, and can thus be fabricated simultaneously with the later type of resonators. Indeed, we have demonstrated the cointegration of both devices, which reveal

to be complementary in terms of applications. This opens the possibility to provide both wide band filtering with SMR and a narrow band filtering with guided wave resonators, which naturally exhibit a lower electromechanical coupling factor. Additionally, various frequencies can be reached simultaneously on the same chip by adjusting the dispersion characteristics of the material stack and fixing the wavelength through the layout of the electrodes.

This work was partly funded by the French Public Authorities through the NANO 2012 program. The authors want to thank the whole ST-LETI BAW team for their help and support. They are also grateful to Dr. Emmanuel Defaÿ from CEA, LETI, and to Didace Ekeom, from Microsonics, for fruitful discussions.

- ¹G. Piazza, P. Stephanou, and A. Pisano, *J. Microelectromech. Syst.* **15**, 1406 (2006).
- ²V. Yantchev and I. Katardjiev, *IEEE Trans. Ultrason. Ferroelectr. Freq. Control* **54**, 87 (2007).
- ³M. Desvergne, E. Defaÿ, D. Wolozan, M. Aïd, P. Vincent, A. Volatier, Y. Deval, and J.-B. Begueret, Proceedings of the 37th European Solid State Device Research Conference, 2007, pp. 358–361.
- ⁴M. Benetti, D. Cannata, F. Di Pietrantonio, and E. Verona, *Proc.-IEEE Ultrason. Symp.* **2007**, 1676.
- ⁵G. Ho, R. Abdolvand, A. Sivapurapu, S. Humad, and F. Ayazi, *J. Microelectromech. Syst.* **17**, 512 (2008).
- ⁶V. Yantchev, L. Arapan, and I. Katardjiev, *IEEE Trans. Ultrason. Ferroelectr. Freq. Control* **56**, 2701 (2009).
- ⁷A. Volatier, G. Caruyer, D. Pellissier Tanon, P. Ancey, E. Defaÿ, and B. Dubus, *Proc.-IEEE Ultrason. Symp.* **2005**, 905.
- ⁸I. Koné, B. Dubus, L. Buchaillot, A. Reinhardt, F. Casset, M. Aïd, J. F. Carpentier, and P. Ancey, Proceedings of the IEEE International Frequency Control Symposium, 2008, pp. 581–585.
- ⁹A. Khelif, A. Choujaa, J.-Y. Rauch, V. Pettrini, H. Moubchir, S. Benchabane, and V. Laude, *Proc.-IEEE Ultrason. Symp.* **2008**, 307.
- ¹⁰R. F. Milsom, F. W. M. Vanheltmont, A. B. M. Jansman, J. Ruigrok, and H.-P. Loebel, "Bulk acoustic wave resonator device," Patent Application No. WO2006126168 (Nov. 2006).
- ¹¹A. Reinhardt, T. Pastureaud, S. Ballandras, and V. Laude, *J. Appl. Phys.* **94**, 6923 (2003).
- ¹²S. Marksteiner, J. Kaitila, G. G. Fattinger, and R. Aigner, *Proc.-IEEE Ultrason. Symp.* **2005**, 329.
- ¹³K. Blotekjaer, K. Ingebrigsten, and H. Skeie, *IEEE Trans. Electron Devices* **20**, 1139 (1973).
- ¹⁴T. Jamneala, U. B. Koelle, A. Shirakawa, S. R. Gilbert, P. Nikkel, C. Feng, and R. Ruby, *IEEE Trans. Ultrason. Ferroelectr. Freq. Control* **56**, 2553 (2009).
- ¹⁵I. Viktorov, *Rayleigh and Lamb Waves: Physical Theory and Applications* (Plenum, New York, 1967).
- ¹⁶G. Fattinger, S. Marksteiner, J. Kaitila, and R. Aigner, *Proc.-IEEE Ultrason. Symp.* **2005**, 1175.